Genetic instability of the tumor suppressor gene FHIT in normal human cells

ARTICLE *in* GENES CHROMOSOMES AND CANCER · SEPTEMBER 2013

Impact Factor: 4.04 · DOI: 10.1002/gcc.22079 · Source: PubMed

4 AUTHORS, INCLUDING:

Elisa Palumbo
University of Padova
8 PUBLICATIONS **116** CITATIONS
SEE PROFILE

Elena Tosoni
University of Padova
4 PUBLICATIONS **36** CITATIONS
SEE PROFILE

Laura Matricardi
Istituto Oncologico Veneto
6 PUBLICATIONS **41** CITATIONS
SEE PROFILE

RESEARCH ARTICLE

Genetic Instability of the Tumor Suppressor Gene *FHIT* in Normal Human Cells

Elisa Palumbo[†,+], **Elena Tosoni**[‡,+], **Laura Matricardi**[§], **Antonella Russo**[*]

Department of Biology, University of Padova, Via U. Bassi 58/b, 35131, Padova, Italy

Common fragile sites are hotspots for chromosome instability and co-localize to cancer genomic rearrangements. Whether these loci may be considered stable in human subjects under physiological conditions remains an open question. Here we show by molecular combing that a small but significant percentage of normal human cells carry an abnormal sequence pattern within the tumor suppressor gene *FHIT* (3p14.2) at *FRA3B*. Each sequence variation represents a unique pattern within a normal cell population, and therefore it would remain undetected or not interpreted by genome-wide analyses. Remarkably, the region is the same as in *FHIT* rearrangements described in tumors. By analyses on several normal cell lines (proliferating and resting primary lymphocytes, primary fibroblasts, lymphoblastoid cells including clonal cell cultures) we verified that: (a) each cell type displays altered sequence patterns at *FHIT*; (b) the presence of abnormal sequence patterns is specific for the *FHIT* locus; and (c) *FHIT* instability occurs *de novo* during cell proliferation, and heterogeneous sequence variants progressively accumulate in the cell populations. *FHIT* has been widely investigated in cancer cells, but to our knowledge this is the first direct evidence of spontaneous and recurrent occurrence of genomic instability at this gene in human subjects, at the same region involved in cancer rearrangements. Our results suggest that common fragile site activity is not restricted to *in vitro* cell culture and that genomic instability may pre-exist in normal cells in the absence of exogenous replication stress. © 2013 Wiley Periodicals, Inc.

INTRODUCTION

FRA3B (3p14.2), the most actively expressed common fragile site of the human genome, encompasses a large region (over 4 Mb) of chromosomal instability (Rassool et al., 1996; Becker et al., 2002) harboring several genes including the Fragile Histidine Triad gene (*FHIT*). *FHIT* is a large gene that extends over about 1.5 Mb. Its large size is related to the presence of very large intronic sequences, a typical feature of genes mapping within common fragile sites (Smith et al., 2006). In particular, introns 4 and 5 are large, respectively, 285 kb and 523 kb; the core of fragility is centered on exon 5 (Ohta et al., 1996; Zimonjic et al., 1997).

FHIT encodes a protein involved in intracellular signaling and DNA damage response (Okumura et al., 2009; Saldivar et al., 2010, 2012). An increasing number of studies indicates that the FHIT protein is absent or reduced in most tumors, including many of the digestive system (from the oral cavity and oesophagus to the colon), and those affecting the pancreas and liver (Okumura et al., 2009). Because FHIT protein appears necessary for correct DNA damage response, the loss of this gene may be the first step on a genomic instability pathway ultimately leading to cell transformation (Saldivar et al., 2010, 2012).

Several chromosomal alterations and rearrangements in cancer cells involve the *FHIT* locus (Okumura et al., 2009), but this observation does not imply a direct causative role of the fragile site in cell transformation, because cancer cells are sometimes genetically unstable *per se*. Moreover, because of the tumor suppressor activity of *FHIT*, the finding of rearrangements in its genomic sequence could simply reflect a preferential positive selection of cells that have lost FHIT function.

About 30 years after the hypothesis was put forward (Yunis and Soreng, 1984) of a possible involvement of common fragile sites in cancer

Additional Supporting Information may be found in the online version of this article.

[+]E. Palumbo and E. Tosoni contributed equally to this work.

[†]Present address: Familial Cancer Clinic and Oncoendocrinology, Veneto Institute of Oncology (IOV-IRCCS); Department of Medical and Surgical Sciences, University of Padova, Via Gattamelata 64, Padova 35128, Italy

[‡]Present address: Department of Molecular Medicine, University of Padova, Via A. Gabelli, 63, 35121, Padova, Italy.

[§]Present address: Veneto Institute of Oncology (IOV-IRCCS), Via Gattamelata 64 35128, Padova, Italy.

Supported by: University of Padova, Department of Biology.

*Correspondence to: Antonella Russo, Department of Biology, University of Padova, Via U. Bassi 58/b, 35131 Padova, Italy.
E-mail: antonella.russo@unipd.it

Received 23 April 2013; Accepted 10 May 2013

DOI 10.1002/gcc.22079

Published online in Wiley Online Library (wileyonlinelibrary.com).

development, the potential relevance of these loci is still debated (Bignell et al., 2010). Moreover, because breakages at common fragile sites are expressed *in vitro* under specific cell culture conditions, one key question is whether these loci may be considered stable in human subjects.

Here we show by molecular combing that in normal human cells a small but significant percentage of abnormal sequence patterns may be found within the *FHIT* gene, at the same genomic region that is involved in many cancer rearrangements. This effect is detectable in different types of proliferating and resting cells, in the absence of exogenous stress. To our knowledge, this is the first direct evidence of recurrent genomic instability at the tumor-suppressor gene *FHIT* in human healthy subjects.

MATERIALS AND METHODS

Cells

Primary human peripheral lymphocytes (PBL) from healthy subjects were isolated from buffy coats provided anonymously from the Blood Transfusion Service, University Hospital of Padova. Subject 1 and subjects 3–5 were males; subject 2 was female. Mononuclear cells were obtained by centrifugation on Ficoll-Paque (HISTOPAQUE 1077, Sigma-Aldrich, Milano, Italy) and resuspended in RPMI 1640 medium supplemented with antibiotics and 10% foetal bovine serum (FBS). PBL were immediately processed for molecular combing, or PHA-stimulated to proliferate, according to standard protocols; they were grown for 48–72 hr before harvest.

Immortalized B lymphoblastoid cells (TK6 and H691) were cultured in RPMI 1640 medium supplemented with antibiotics and 10% FBS. Duplication time is 24–30 hr for both cell lines.

IMR-90 cells (a diploid fibroblast strain derived from foetal lung) were grown in DMEM medium supplemented with antibiotics and 10% FBS. Cultures started from independent frozen samples of cells at low population division (PD) were harvested at different PD in the range 21–37.

All culture reagents were obtained for Gibco, Life Technologies, Monza, Italy.

Molecular Combing

Exponentially growing cells were harvested and immobilized in agarose plugs as described in detail elsewhere (Palumbo et al., 2010). Plugs with resting PBL were prepared immediately after isolation from the mononucleated fraction. After overnight treatment with Proteinase K (50°C; 2 mg/ml in digestion solution: 0.01 M Tris-HCl, pH 8, 0.02 M NaCl, 0.1 M EDTA, 1% N-Laurosylsarcosine), plugs were washed and permanently stored in 0.5 M EDTA, pH 8.0 at 4°C. High molecular weight DNA was obtained by digesting 1–2 plugs with β-agarase (3 U, New England BioLabs, EuroClone, Pero, Milano, Italy) in 0.1 M MES, pH 6.5. DNA combing on silanized surfaces was done according to a standard procedure. More details are provided in Palumbo et al., 2010.

Single-Locus Analysis on Combed DNA

BAC genomic clones (Children's Hospital Oakland Institute—CHORI, Oakland, CA) detecting *FRA3B*, *LAMINB2*, and *FRA6E* loci (Fig. 1) were labeled by random priming (BioPrime DNA labeling System, Invitrogen, Life Technologies). The labeling kit provides biotin-labeling of probes; a custom-made reaction nucleotide mix containing digoxigenin-11-dUTP (Roche Applied Science, Monza, Italy) was used to achieve the differential labeling of probe pairs.

Per each slide the hybridization mix consisted of: 250–300 ng of each labeled probe, 13X-17X Cot-1 DNA (Invitrogen, Life Technologies), 10 μg of Salmon sperm DNA (Invitrogen, Life Technologies). Combed DNA was denatured in 1 M NaCl, 50 mM NaOH for 15 min and dehydrated in 70%, 90%, and 100% ethanol solutions (3 min each). In parallel, the cocktail of probes was denatured at 80°C for 10 min. Twenty microliters were applied onto denatured preparations, which were covered with a 22 × 22 mm coverslip, sealed with rubber cement, and incubated overnight at 37°C in a humidified chamber. Stringency washes were: 3 × 5 min 50% formamide, 2× SSC, pH 7.0; 3 × 5 min 2× SSC, pH 7.0.

The biotin-labeled probe was detected by 594 Alexa Fluor-conjugated streptavidin (1:50, Molecular Probes, Life Technologies), followed by polyclonal biotin-conjugated antistreptavidin antibodies (1:50, Rockland Immunochemicals, tebu-bio, Magenta, Milano, Italy), and a third layer of 594 Alexa Fluor-conjugated streptavidin (1:75, Molecular Probes, Life Technologies). Simultaneously, to detect the digoxigenin-labeled probe a mouse monoclonal antidigoxigenin antibody (1:25, Roche Applied Science) and a 488 Alexa Fluor-conjugated anti mouse IgG made in goat (1:50, Molecular Probes, Life Technologies) were used in the first and second layers, respectively.

Preparations were mounted for microscope analysis with Vectashield (Vector, DBA, Segrate, Milano, Italy).

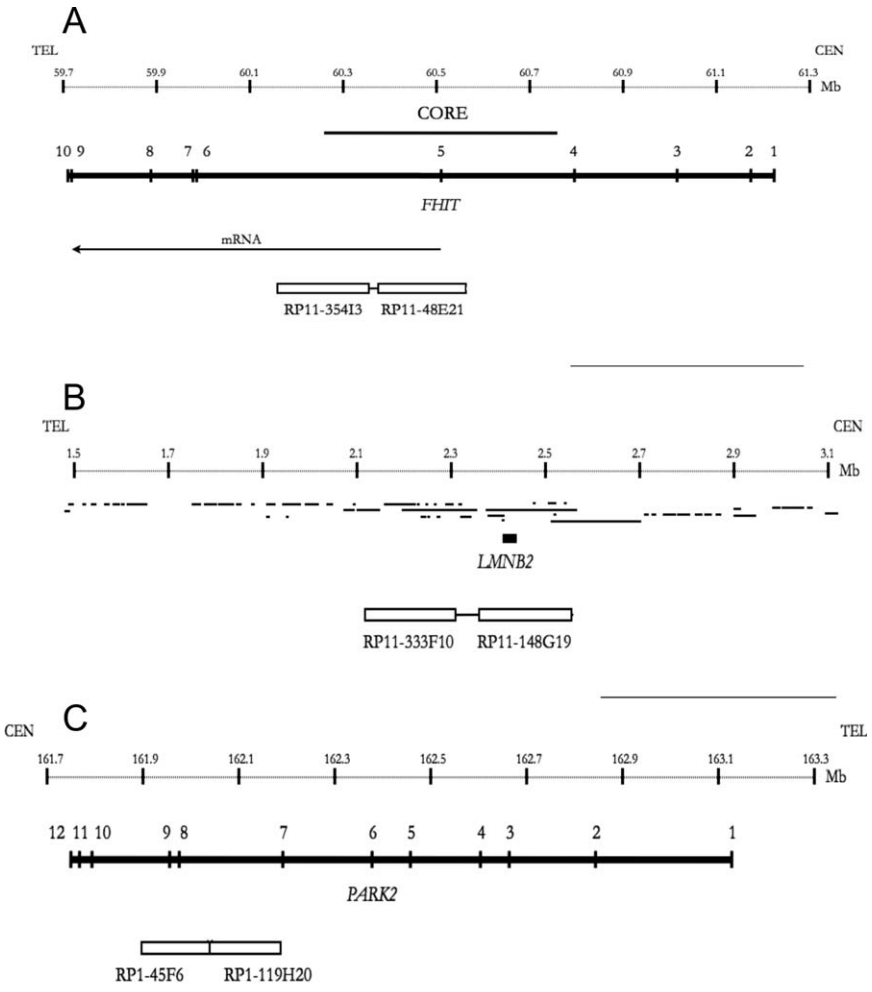

Figure 1. The genomic regions investigated: black lines represent genes, white segments correspond to probes used in molecular combing experiments. Calibration bar = 500 kb. (A) At *FRA3B*, BAC clones RP11–354I3 and RP11–48E21 identify a sequence of about 450 kb centered at the fragility core of the long *FHIT* gene, here represented with its exon/intron organization. Probe-to-probe distance, estimated on PHA-PBL, is 18.4 ± 0.22 kb (348 observations). (B) The nonfragile region is a sequence centered around the early replicating gene *LAMINB2* (*LMNB2*, thick black line) and identified by two adjacent probes (BAC clones RP11–333F10 and RP11–148G19) spaced 46.7 ± 0.44 kb (98 observations on PHA-PBL); several additional genes present in the region are represented by thin black lines. (C) At *FRA6E*, probes RP1–45F6 and RP11–119H20 with expected null distance were used. The probe pair identifies the fragility core of the fragile site, within the long gene *PARK2* (here represented with its exon/intron organization).

Image Analysis

Combed DNA was scored under a 40× oil immersion objective (N.A. = 1.30) by using a motorized fluorescence microscope (Zeiss Axio Imager.M1, Carl Zeiss, Milano, Italy) equipped with a CCD camera (Photometrix, CoolSNAP HQ^2, Crisel Instruments, Roma, Italy). In order to collect images of complete DNA molecules, which span multiple microscope fields, single wavelength-images acquired under adequate filter sets were merged. Images of adjacent fields were then aligned using Adobe Photoshop CS2, and the Metavue software (Crisel Instruments) was used to obtain measurements of the fluorescent signals of interest. According to the molecular combing calibration factor (1 μm = 2 kb) and to the magnification features of the objective and the CCD camera, 1 pixel = 0.16125 μm = 0.3225 kb.

Because the combed genomic DNA is not counterstained, molecules were discarded if linear fluorescent signals did not follow a linear array, and in all additional situations where the fluorescent patterns could not be attributed with maximum confidence to a single molecule. Patterns of hybridization were evaluated by measuring the length of hybridization signals and the probe-to-probe distances (Supporting Information Fig. 1).

Transcription Analysis

Total RNA from resting and PHA-stimulated lymphocytes, lymphoblastoid cell lines (TK6 and H691), and human primary fibroblasts (PD 29–35) was isolated with Trizol (Invitrogen, Life Technologies). Reverse transcription was carried out at 42°C for 60 min, in a reaction volume of 25 μL containing 500 ng of total RNA. Three microliters of cDNA were used as template for PCR reactions with the following primer pairs:

FHIT_Ex1–9 (expected product 640 bp):

For.: 5'-TTTCATTCCCAGCTGTCAACA-3'; Rev.: 5'-TCCTCTGATCTCCAAGAGGC-3'

FHIT_Ex4–6 (expected product 198 bp):

For.: 5'-CCGAAGAGGTAGCAGTCTTCTG-3'; Rev.: 5'- ACGCAGGTCATGGAAGC-3'

GAPDH (expected product 143 bp):

For: 5'-CCTCAACGACCACTTTGTCA-3'; Rev: 5'-TTCCTCTTGTGCTCTTGCTG-3'

PCR conditions, slightly adjusted for each sequence, consisted in: 94°C for 5 min, followed by 31 or 35 cycles at 94°C for 30 sec, 55–60°C for 30 sec, and 72°C for 15–45 sec; final extension step: 72°C for 1–3 min.

RESULTS

Altered *FHIT* Sequences can be Detected in Normal Proliferating Cells

By molecular combing DNA molecules are elongated at constant force, and after fluorescent *in situ* hybridization the spatial arrangement of different probes reflects real distances along the molecule (Michalet et al., 1997). By applying this methodology we aimed to evaluate the occurrence of small scale sequence alterations at *FHIT*, the fragility core of *FRA3B*, within a population of normally proliferating cells. Different cell types were considered, namely: PHA-stimulated peripheral blood lymphocytes (PBL) from four different healthy subjects, primary human fibroblasts (the strain IMR-90), and immortalized B lymphocytes (cell lines TK6 and H691). Two-color FISH with probes targeting the fragility core of *FRA3B* (RP11–354I3 and RP11–48E21, Fig. 1A) was applied.

In all cell samples the spatial pattern of the two hybridization signals was rather variable, a result which is in contrast with the expectations of the molecular combing technique; probe-to-probe distances ranged in wide intervals (Figs. 2A and 2B), and most importantly abnormal patterns of the two probes were recorded, consisting in the merging of the two fluorescent linear hybridization signals (Fig. 2C). Merging patterns were of variable extension, from a minimum involvement of 4.8 kb to a maximum of 153.7 kb, and each of them represented a unique variation within and among the cell populations investigated. Finally, a rearranged molecule carrying a sequence duplication was detected in a PBL sample (Fig. 3).

The frequency of molecules with merging patterns ranged among the different cell types investigated (1.9–14.3%), but importantly, the overall proportion of these patterns was highly reproducible within replicated experiments (cells from the same line, grown and harvested in independent trials; Table 1). Only for H691 cells, two independent analyses gave heterogeneous results (1.9% and 6.3% of merging patterns, respectively; Table 1). A possible interpretation for this variation was that in the first analysis harvesting and DNA preparation occurred at a rather short time interval after recovery from frozen state (less than 15 days). This unusual condition could have played a role in introducing some clonal effect in the initial phase of H691 cultures (which start from frozen samples in 24-well plates) before the massive proliferation activity. Interestingly, the value observed in the first analysis with H691 cells was not only lower than that in the replicated experiment, but it also represented the lowest observation among all cell lines. Overall, merging patterns were less frequent in fibroblasts than in PBL/lymphoblastoid cells ($P < 0.001$).

All the abnormal patterns observed map in the *FHIT* region encompassing the core of instability of the fragile site.

Merging Patterns are a Specific Feature of the FHIT Sequence

In the above set of data, two elements support a biological basis for the merging patterns: the strict reproducibility of their frequencies within the same cell line, and the observation that different cell types are characterized by a diverse proportion of merging patterns. In order to provide adequate controls and to exclude the contribution of possible artefacts, additional genomic regions were evaluated by the same two-color FISH approach, using probe pairs with spatial arrangements comparable to the *FHIT* probes. In particular, a non-fragile region, harbouring the early replicating gene *LAMINB2* and several other coding sequences (hence referred to as the *LAMINB2* locus, Fig. 1B), as well as the fragility core of a different common fragile site (*FRA6E*) harbouring

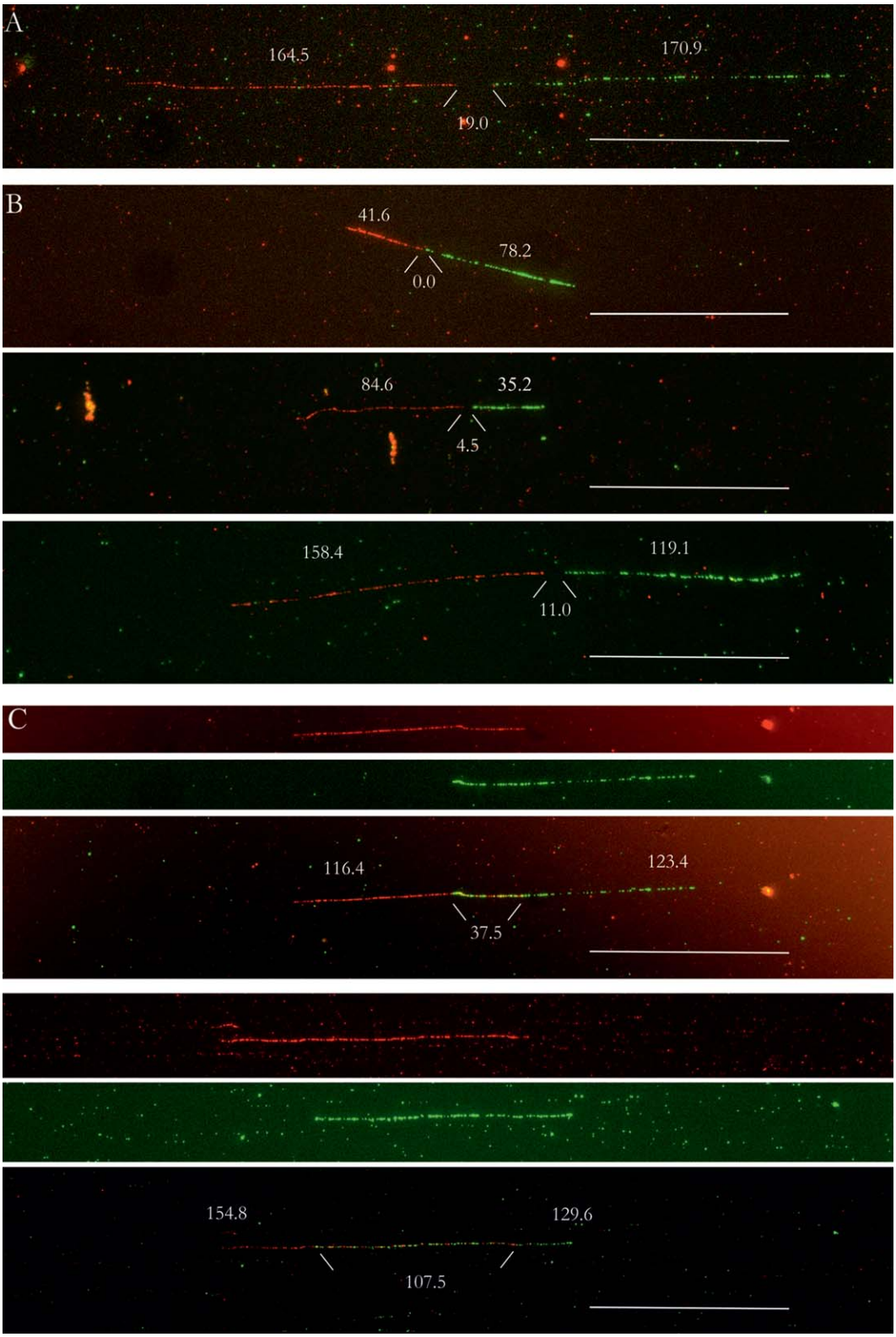

Figure 2. Representative images of the *FHIT* locus as detected by FISH and molecular combing. The length of each probe and their relative distance (or the extension of a merging pattern) are indicated in kb. Calibration bar = 100 kb. (A) The normal hybridization pattern expected for probes RP11–354I3 (red) and RP11–48E21 (green); (B) Molecules showing probe-to-probe distances deviating from normal values; (C) Two examples of molecules with a merging sequence pattern: top to bottom the hybridization signals detected at each specific wavelength are shown, followed by the merging image of each molecule.

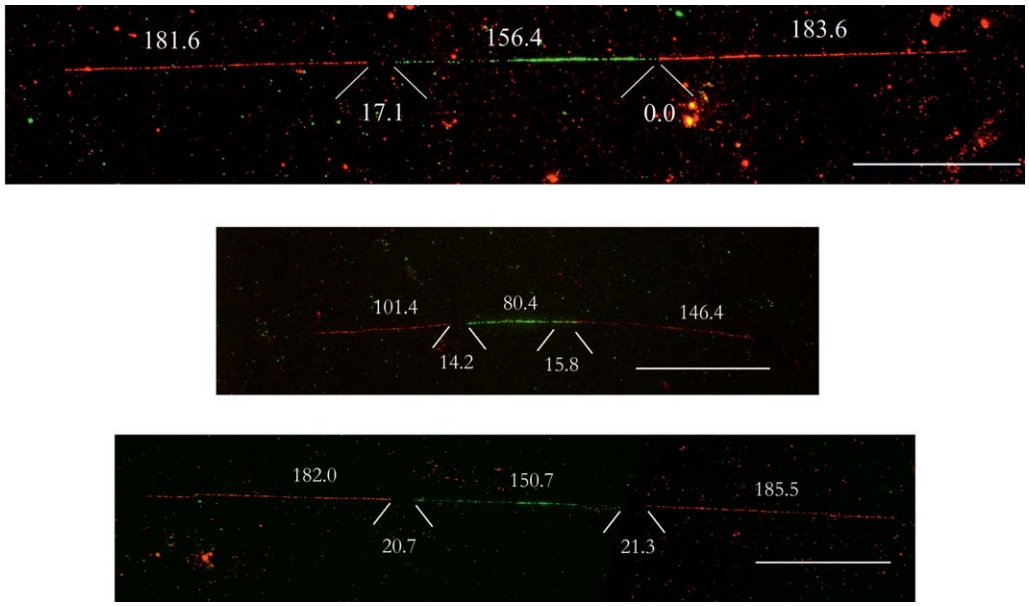

Figure 3. The three cases of duplication observed in this study at *FHIT*. The length of each probe, their relative distance (or the extension of a merging pattern) are indicated in kb. Calibration bar = 100 kb. Top: a rearranged molecule observed in PHA-PBL from subject 4. The two probes RP11–354I3 (red) and RP11–48E21 (green) are seen in their expected spatial pattern on the left, while on the right a second copy of probe RP11–354I3 (red) is detected immediately downstream probe RP11–48E21 (green). This molecule should be interpreted as a tandem duplication; one boundary of the duplicated segment involves the telomeric segment of clone RP11–48E21, but the actual extension of the duplication is unknown. Notably, because the length of the green probe is less than expected, although located in the inner segment of the combed molecule, a deletion must be present adding complexity to this rearranged molecule. Middle: one rearranged molecule observed in the TK6 clonal population B. On the left, two probes with normal alignment are separated by shorter distance than expected; in addition, downstream on the same molecule a second copy of RP11–354I3 (red) is present with a merging pattern (yellow fluorescence). Bottom: one rearranged molecule observed in the TK6 clonal population D. The two probes on the left are adjacent to a second copy of RP11–354I3 (red, on the right); both probe-to-probe distances are in slight excess with respect to the expected range.

the *PARK2* gene (Fig. 1C), were analyzed. Remarkably, for this second fragile site an extreme condition was considered: two probes hybridizing contiguously, i.e. with expected distance 0. For the best rigorous comparisons, these analyses were carried out on DNA combed from the same preparations previously used for the *FHIT* data set.

At the nonfragile *LAMINB2* locus the probe-to-probe distances estimated on PBL and H691 cells (Supporting Information Table 1) were consistent with the expected value (Figs. 1B and 4A, 4C). In consideration of the resolution of the molecular combing (about 5 kb), the deviations around the mean value fall in the normal range (Fig. 4C).

TABLE 1. Structural Analysis of *FRA3B* Fragility Core in Several Proliferating Cell Types, as Evaluated by Two-color FISH in Replicated Experiments

Cell sample	Total probe pairs	Normal patterns	Probe to probe distance (kb) (mean ± SE)	Median (kb)	Min distance (kb)	Max distance (kb)	Merging patterns		Size of merging patterns (kb)	
							N	%	Min	Max
PHA-PBL Subject 1	30	26	18.6 ± 0.51	17.8	14.6	37.2	4	13.3	75.0	136.5
PHA-PBL Subject 2	70	60	18.0 ± 0.51	17.8	10.0	31.0	10	14.3	12.8	122.9
PHA-PBL Subject 3	221	196	18.6 ± 0.26	18.4	9.7	34.2	25	11.3	10.2	149.3
PHA-PBL Subject 4	74	67	17.5 ± 0.63	17.6	0.0	34.4	7	9.5	4.8	72.8
TK6 I analysis	110	98	19.6 ± 0.80	17.8	0.0	53.8	12	10.9	17.2	152.3
TK6 II analysis	126	113	17.6 ± 0.40	17.4	0.0	29.5	13	10.3	7.5	76.0
H691 I analysis	106	104	19.7 ± 0.31	18.7	13.2	27.4	2	1.9	58.5	70.7
H691 II analysis	95	89	17.6 ± 0.41	17.1	10.0	36.2	6	6.3	19.1	153.7
IMR-90 PD 21	154	151	16.8 ± 0.31	16.5	10.3	35.2	3	1.9	20.7	85.3
IMR-90 PD 23	110	107	16.4 ± 0.40	16.0	0.0	28.7	3	2.7	47.7	78.4

The expected spatial organization of probes is shown in Figure 1A.

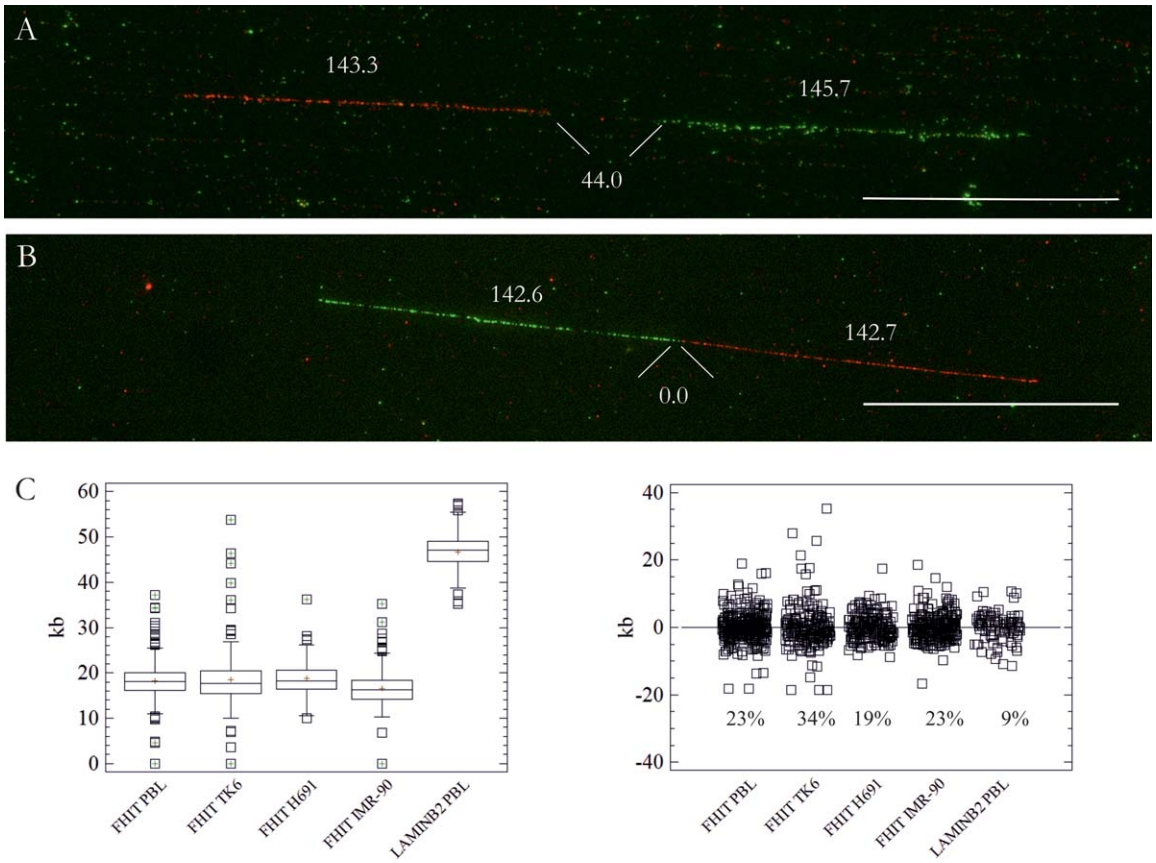

Figure 4. Representative images from structural analysis at *LAMINB2* and *FRA6E* loci by molecular combing. The length of each probe and their distance are indicated (kb). Calibration bar = 100 kb. (A) The normal hybridization pattern for probe pair RP11–333F10 (red) and RP11–148G19 (green) at *LAMINB2*. (B) At *FRA6E*, RP1–45F6 (green) and RP11–119H20 (red) hybridize contiguously. (C) Left panel: box-plot diagrams of the probe-to-probe distances estimated at *FHIT* and *LAMINB2* in several cell types. Data from Table 1 and Supporting Information Table 1 were elaborated with the software Statgraphics. Outliers, represented by symbols filled with a plus sign, are detectable in all data distributions concerning *FHIT* but are absent from the data collected at *LAMINB2* locus. Right panel: a comparison of deviations of single distances from the mean value representing each locus and cell sample confirms the existence of largest heterogeneity at the *FHIT* locus than at *LAMINB2*. Per each distribution the coefficient of variation (percentage) is indicated.

Raw data from *FHIT* (Table 1) and *LAMINB2* (Supporting Information Table 1) were elaborated with the software Statgraphics. For distance distributions evaluated at *FHIT* in the different cell lines the coefficient of variation was two-fold higher than that for *LAMINB2* (Fig. 4C), and only *FHIT* data were characterized by the presence of outliers (Fig. 4C). Furthermore, merging patterns were not observed at the *LAMINB2* region. Also at *FRA6E*, where two probes should hybridize contiguously on DNA molecules (Fig. 1C), only the expected sequence pattern with distance 0 was observed (Supporting Information Table 1, Fig. 4B).

Because the spatial arrangement of probe pairs was never altered in the two genomic regions considered in these comparisons, we interpreted our observations at *FHIT* as specific indicators of instability at the fragility core of *FRA3B*, in the absence of aphidicolin-induced replication stress.

Merging Patterns are also Visible in Resting Cells and Pre-exist In Vivo

PBL isolated from two different donors (subjects 3 and 4) were evaluated before and after PHA stimulation, in order to rule out that merging patterns occur during the cell proliferation *in vitro*. A fraction of resting cells was immediately processed for molecular combing and analyzed by two-color FISH. The remaining cells were PHA-stimulated to proliferate before DNA molecular combing (these samples contributed to data listed in Table 1). It appeared that in resting and proliferating PBL of the same subject both the frequency and the extension of the unexpected sequence patterns at *FHIT* were strictly comparable (Supporting Information Table 2; Fig. 5). It can be concluded that *FHIT* genomic instability pre-exists *in vivo* in PBL of human healthy subjects.

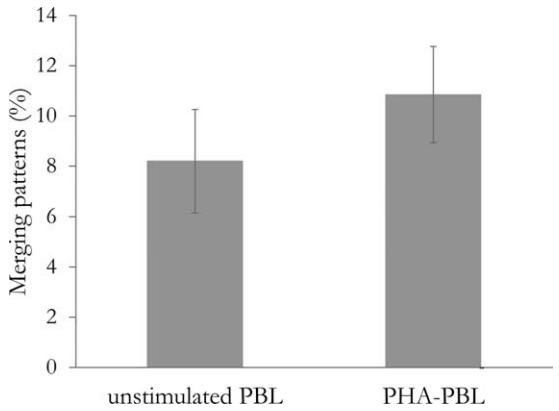

Figure 5. Pooled percentages of merging patterns detected in unstimulated and stimulated (PHA-PBL) lymphocytes of two healthy donors. Error bar = SE of the percentage. Data from Supporting Information Table 2.

Genomic Instability at FHIT may be Modulated by Cell Proliferation

Human primary fibroblasts (IMR-90) harvested at PD 21–23 showed the lowest percentage of merging patterns among the cell types evaluated (Table 1). To understand the possible link between cell proliferation and origin/accumulation of aberrant sequence patterns, independent cultures of IMR-90 cells (set up from low PD frozen samples) were grown, respectively, up to PD 35 or 37. Merging patterns were significantly more represented at PD 35–37 (8.5%) than at PD 21–23 (2.3%) ($P < 0.01$, Fig. 6; Supporting Information Table 3), thus suggesting that sequence instability may be modulated by the cell proliferation activity. The consistency of the observed difference is supported by the high reproducibility of data from replicated experiments (Supporting Information Table 3). It is important to remark that primary fibroblasts are still actively proliferating at late PD, as judged by the unchanged percentage of BrdU-labeled nuclei at PD 21–23 versus 35–37 (data not shown).

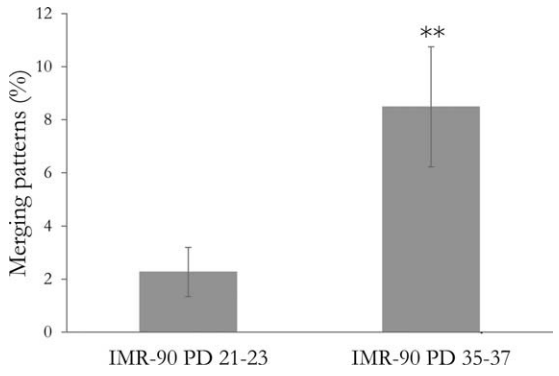

Figure 6. Merging pattern frequencies detected in IMR-90 cells at increasing population doublings (PD). ** $P < 0.01$; Error bar = SE of the percentage. Data from Supporting Information Table 3.

Origin and Transmission of Abnormal Patterns in Clonal Cell Progeny

Although abnormal sequence patterns represented 1–10% of the observed cell sample, each molecule carrying a sequence abnormality at *FHIT* corresponded to a unique pattern within the cell population of origin. In addition, according to IMR-90 data the overall frequency of merging patterns increases in a proliferating cell population. To better understand the fate and evolution of the observed merging patterns at *FHIT*, we attempted the analysis of clonal cell cultures. Figure 7A summarizes the rationale of this experiment: a normal cell must generate a normal cell progeny, but sequence variations can be formed *de novo* during proliferation. Thus, in a clonal cell culture the abnormal patterns, if observed, should be present at a rather low frequency. Alternatively, a cell already carrying a sequence variation (rare in the

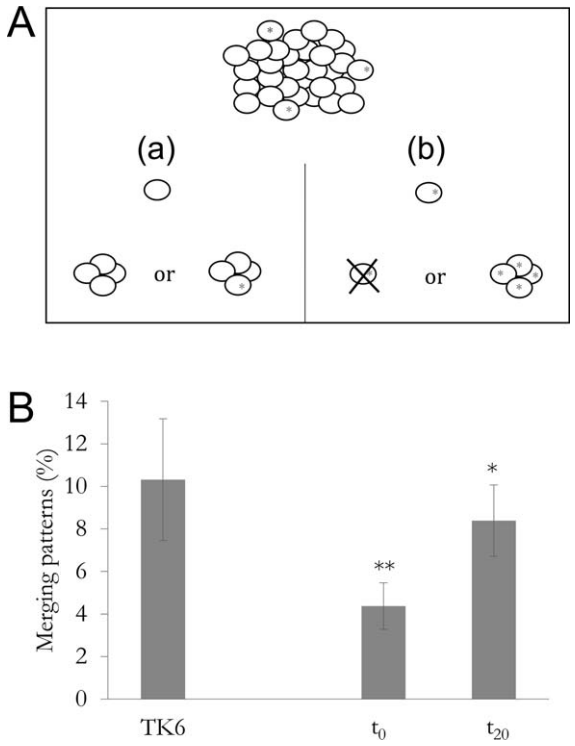

Figure 7. (A) the rationale for the analysis of TK6 clonal cell progeny. (a) A normal cell is expected to generate a clonal population lacking sequence abnormalities (on the left), but de novo abnormal patterns (*) can accumulate during cell proliferation (on the right). These abnormalities should remain at rather low frequency in the clonal progeny. (b) A rare cell carrying the altered pattern (*) could be not successful in generating the cell clone (on the left), but when able to proliferate it should transmit the same sequence abnormality to its clonal cell progeny (on the right). (B) merging pattern frequencies in TK6 cells (II analysis of Table 1) and in the pool of 4 clonal populations harvested at two time intervals (t_0 and t_{20}; raw data in Table 2). ** $P < 0.01$ (TK6 vs t_0); * $P < 0.05$ (t_0 vs t_{20}); Error bar = SE of the percentage.

TABLE 2. Structural Analysis of *FRA3B* Fragility Core in Four Independent TK6 Clonal Cultures (A–D) at Different Time Intervals of Growth

Cell sample	Time interval	Estimated population doublings after plating	Total probe pairs	Normal patterns	Probe to probe distance (kb) (mean±SE)	Median (kb)	Min distance (kb)	Max distance (kb)	Merging patterns		Size of merging patterns (kb)	
									N	%	Min	Max
Starting TK6 population[a]			126	113	17.6±0.40	17.4	0.0	29.5	13	10.3	7.5	76.0
Clone A			96	90	18.9±0.42	18.3	11.0	29.8	6	6.3	69.6	127.9
Clone B	t_0	27–30	79	76	16.8±0.31	16.1	11.3	23.7	3	3.8	15.8	60.0
Clone C			82	78	17.8±0.48	17.4	0.0	32.4	4	4.9	5.2	102.6
Clone D			109	106	18.0±0.42	17.8	8.9	36.8	3	2.8	42.9	59.2
Clone A			89	80	18.2±0.36	18.5	11.0	27.5	9	10.1	8.4	124.8
Clone B	t_{20}	43–50	69	62	19.2±0.42	19.0	13.2	27.1	7	10.1	5.2	93.4
Clone C			38	37	20.2±0.79	19.0	14.2	37.8	1	2.6	26.1	–
Clone D			102	94	17.9±0.45	17.7	0.0	35.8	8	7.8	7.1	108.0

The expected spatial organization of probes is shown in Figure 1A.
[a]Data already shown in Table 1 (TK6, II analysis).

starting population) could not be successful in generating a cell clone or, if able to proliferate, the same abnormal pattern should be transmitted to its clonal cell progeny. In this very rare occurrence, the proportion of cells carrying the abnormality should approach 100%.

Fifty nine independent clonal cultures were set up from TK6 cells; cell clones were subcultured and harvested for molecular combing at two time intervals ($t_0 = 18$ days after plating; t_{20} = further 20 days of proliferation). Four cell clones randomly selected were analyzed by two-color FISH to evaluate the presence of merging patterns. At t_0 merging patterns were present at significantly lower frequency than in the starting cell population ($P < 0.01$; Table 2). At t_{20}, a two-fold increase of abnormal molecules was detected with respect to the previous time interval ($P < 0.05$ on the pool of four analyses; Fig. 7B; Table 2). As in the previous analyses, each pattern was unique within the observed sample. The predominant proportion of normal molecules allowed us to conclude that each cell clone was established from a normal cell, and that instability at *FHIT* occurred during cell proliferation leading to a progressive accumulation of sequence abnormalities. Two additional cases of duplication involving the fragility core of *FRA3B* were detected in the course of this analysis, in two different clonal samples (Fig. 3).

FHIT Transcription could be a Contributing Factor to the Onset of Aberrant Molecules

Recent data demonstrated that CFS instability may be based on spatial and temporal overlapping of replication and transcription (Helmrich et al., 2011), and because of the observed variations in the frequencies of merging patterns at *FHIT*, we wondered whether this gene was transcriptionally active in all the cell lines investigated. Furthermore, while published information concerning *FHIT* transcript variants in tumor cells is continuously updated, for normal samples only early expression data are available (Ohta et al., 1996; Druck et al., 1997; Gayther et al., 1997; Panagopoulos et al., 1997; Matthews et al., 2001). Rare variants could have remained unnoticed in the former analyses, and therefore we considered important to assay this aspect with respect to the genomic alterations described before.

By semiquantitative RT-PCR, we confirmed that *FHIT* is expressed in both resting and proliferating primary lymphocytes, as well as in lymphoblastoid cell lines TK6 and H691 (Fig. 8A). In IMR-90 fibroblasts the transcript was barely detected with the maximum number of amplifications applied in our experiments; this suggests a rather low level of expression in this cell type, previously found to carry the lowest proportion of merging patterns. Remarkably, a positive trend along PD could be appreciated both for the proportion of merging patterns and for the transcriptional activity at *FHIT* (Fig. 8A). Finally, to exclude the possible presence of aberrant transcripts in normal cells, the observations based on the above primer pair, which amplifies a large sequence of *FHIT* mRNA (exons 1–9, 640 bp), were completed by further evaluations focusing on the specific region involved in genomic instability (exons 4–6, 198 bp) (Fig. 8C). Under our

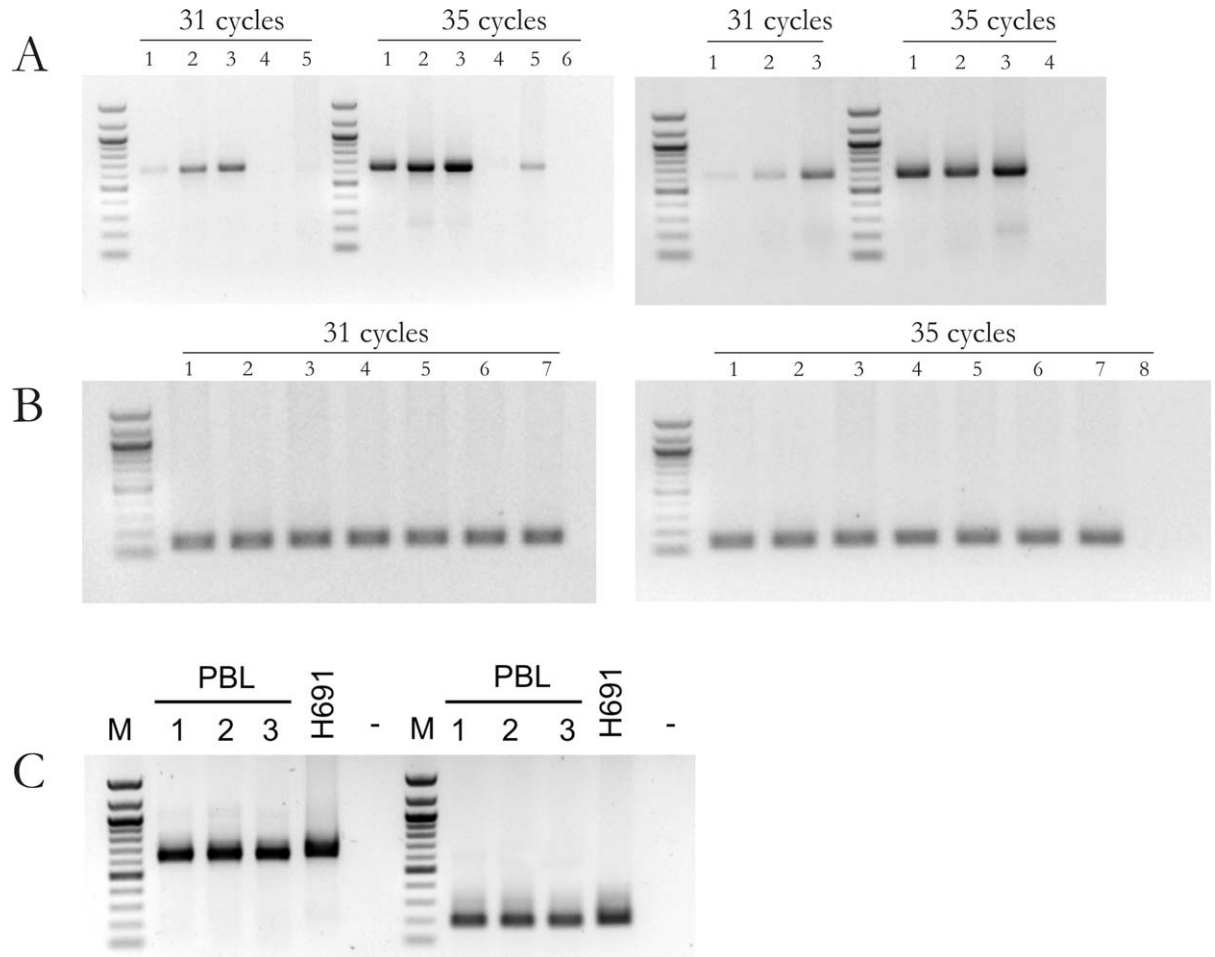

Figure 8. (A) *FHIT* expression in the different cell types used in the study, as evaluated by semiquantitative RT-PCR; the product corresponds to exons 1–9 (640 bp). Left panel: Resting PBL (1), TK6 cells (2), H691 (3), IMR-90 PD 29 (4), and IMR-90 PD 35 (5); 6 = negative control. Right panel: Resting PBL (1–2) and PHA-PBL (3); 4 = negative control. (B) GADPH expression (positive control) in resting PBL (1–2), PHA-PBL (3), TK6 cells (4), H691 cells (5), IMR-90 PD 29 (6), IMR-90 PD 35 (7); 8 = negative control. (C) No altered FHIT transcripts are detected by RT-PCR in PBL samples from three human subjects and in H691 cells. Left: exons 1–9 (640 bp); right: exons 4–6 (198 bp). - = negative control; M = 100 bp ladder.

conditions, only the normal products were observed in PBL sampled from three healthy subjects and in H691 cells; we concluded that the aberrant sequence patterns are not contributing to detectable aberrant *FHIT* transcripts.

DISCUSSION

The instability of common fragile sites is well described in cell culture under replication stress conditions (Durkin and Glover, 2007; Pichiorri et al., 2008); whether these loci may be considered stable in human subjects under physiological conditions is a fundamental question to understand their actual relevance for cancer. Here we provide evidence of the intrinsic *in vivo* instability of *FHIT* genomic sequence at the fragility core of *FRA3B:* in different normal cell types, in the absence of aphidicolin-induced replication stress, abnormal patterns showing wide variations of the expected probe-to-probe distance were observed; among these, few molecules were found with joined hybridization signals (i.e. distance 0; Fig. 2B). In addition, three cases of sequence duplications were observed (Fig. 3). These observations would suggest a frequent occurrence of deletions/insertions at the fragility core of *FRA3B* in normal cells. The most prevalently altered patterns at *FRA3B* were, however, the long stretches of merging signals from two adjacent probes, and this complex genomic architecture cannot be explained by classical mechanisms of chromosome rearrangement.

Different elements contribute to exclude technical artefacts, and to conclude that the observed merging patterns represent frank sequence abnormalities occurring specifically at *FHIT:*

First, they are observed in highly reproducible proportions within replicated experiments, but in contrast their frequency is different among the cells types evaluated (Table 1). Second, they were never observed in our previous experience with molecular combing (Palumbo et al., 2010), furthermore in this study we demonstrated that only normal hybridization patterns are observed at a nonfragile genomic region (*LAMINB2*) and at a second CFS (*FRA6E)* (Supporting Information Table 1). Third, abnormal patterns are present in resting PBL, with percentages strictly comparable to those observed in PHA-stimulated PBL from the same subjects (Supporting Information Table 2). This observation leads to two important conclusions: (a) the abnormal patterns might not have simply arisen during *in vitro* PBL culture, but they pre-existed *in vivo*; and (b) in these molecular combing preparations abnormal patterns cannot be merely attributed to an improper visualization of secondary structures associated to the replicating DNA. Fourth, according to replicated experiments carried out in independent cultures of primary fibroblasts, the fraction of merging patterns is increasing along PD (Fig. 6), an observation suggesting that the aberrant molecules are the product of dynamic events arising in the course of the proliferation activity; data collected on clonal cell populations (Fig. 7B) reinforce this concept.

The sequence abnormalities detected in this study should correspond to a large intronic region and involvement of exon sequences would be rather improbable (Fig. 1A). Furthermore we did not find evidence of aberrant *FHIT* transcripts in normal cell cultures (Fig. 8). Thus, cells carrying abnormal DNA sequences should express normal mature transcripts, and negative selection should not affect them.

As a result of the variable extension of the anomalies recorded (from 4.8 to 153.7 kb), each of them reasonably corresponding to a unique pattern in a large cell sample, their sequence characterization was not feasible. Indeed, in spite of the great potential of next generation sequencing approaches, which allowed great advances in detecting somatic mosaicism (Jacobs et al., 2012; Laurie et al., 2012) the identification of a single-locus, unique variant, within a population of normal molecules would not be practically affordable. To understand the origin and the biological relevance of the observed aberrant patterns, TK6 clonal populations were generated and followed up; the presence of nonclonal abnormal patterns, and the fact that they increase in proportion along cell generations, indicated that instability at *FRA3B* occurs during normal cell proliferation, and may cause a progressive accumulation of heterogeneous sequence abnormalities in the clonal cell populations (Table 2; Fig. 7). Interestingly, the above results offer the possibility to confirm our explanation for discordant data obtained in replicated experiments with the lymphoblastoid cell line H691 (Table 1): in the first analysis with those cells, merging patterns could have been modulated by a stochastic event during some of the many passages from the generation of frozen cell samples to the recovery of a new cell subpopulation; the difference with respect to an independent cell sample could have been enhanced because the rather short proliferation period did not allow an intense generation of altered patterns.

The relationship between *FRA3B* instability and DNA replication is well known (Le Beau et al., 1998; Wang et al., 1999) and by recent studies it has been clarified that at *FRA3B* both scarcity of initiation sites and weak origin activity apply (Palakodeti et al. 2010; Letessier et al. 2011; our unpublished data). Remarkably, the region involved is the same as the sequence abnormalities observed here. Genomic rearrangements can be generated during DNA replication and replication stress, with several pathways contributing to the restart of stalled/collapsed forks (Branzei and Foiani, 2010; Lambert and Carr, 2013). MM-BIR (Microhomology-Mediated BIR) (Smith et al., 2007; Hastings et al., 2009), a replication-based mechanism predicting the production of complex rearrangements during repeated cycles of long-range strand invasion and template switch, could be involved in the formation of aberrant sequence patterns observed at *FHIT*, where according to BLAST there is no extensive sequence homology; in agreement with the prediction of this model, the linear merging signals would correspond to a DNA segment that has repeatedly recombined and that finally can be recognized by short elements deriving from both probes of the original sequence. Unfortunately, because of the complexity of the pathways involved in the response to replication stress, and the increasing number of crosstalking proteins involved, dissecting the molecular mechanisms underlying the rare sequence abnormalities we have observed at *FRA3B* is not immediately practicable.

Instability of fragile sites may be differentially expressed in different cell types; in particular, breakage at several common fragile sites including *FRA3B* is less frequent in fibroblasts than PBL/lymphoblastoid cells (Murano et al., 1989; Caporossi et al., 1995; Letessier et al., 2011). Also the abnormal sequence

patterns at *FRA3B* described in this study are represented with different frequencies among cell populations, and the lowest proportion has been observed in the fibroblast strain IMR-90, at low PD (Table 1). It has been recently proposed that *FRA3B* fragility is associated to a clash between transcription and replication machineries (Hellmrich et al., 2011), an observation that introduces novel questions about the mechanisms of instability acting at common fragile sites (Debatisse et al., 2012). Interestingly, among the cell types investigated in the present study, the transcriptional activity of *FHIT* is particularly low in primary fibroblasts (Fig. 8A). Coherent with this parallelism, at increasing PD IMR-90 cells display a great number of abnormal sequence patterns (Fig. 6), and a slight increase of transcriptional activity (Fig. 8A). These observations underscore the importance to consider the mutual role of replication and transcription with respect to genome instability (Bermejo et al., 2012).

Different studies on tumor cells demonstrated the presence of *FHIT* deletions or rearrangements in the same region analyzed here (the core of fragility at *FRA3B*) (reviewed in Saldivar et al., 2010). Both extension and position of the genomic variations observed in the present study in normal cells are comparable to those of the *FHIT* deletions generated in a human–mouse somatic hybrid cell line under replication stress, and to those detected in tumors (Durkin et al., 2008). With respect to our hypothesis that MM-BIR could be involved in the generation of abnormal sequence patterns at *FHIT*, it is also worth noting that in the study by Durkin et al. (2008) the only sequence feature that could be related to the origin of deletions was indeed microhomology. Moreover, in Barrett esophagus (a preneoplastic lesion) LOH is present at *FHIT* in the large majority of patients, and the effect is restricted to a region of about 400 kb encompassing exons 4 and 5 (Lai et al., 2010). In the same study, temporal evolution of the rearrangements at *FHIT* sequence has been suggested, and the parallelism with our observations of genomic instability, occurring in normal cells at the same location, is remarkable.

In this frame, it is noteworthy that an increase of PHA-induced breakages at *FRA3B* has been reported in PBL in correlation with the smoking activity of human donors (Stein et al., 2002). The effect is strictly associated to actual tobacco exposure, because chromosome breaks at *FRA3B* have comparable frequencies if PBL are derived from former smokers or from non-smokers (Stein et al., 2002). In the present study, PBL samples were provided anonymously from the Blood Transfusion Service of the University Hospital, and information concerning the smoking activity of the donors was not available. The possibility that tobacco can enhance the spontaneous instability seen at *FHIT* in the absence of exogenous stress represents an interesting aspect to be addressed in further investigations.

The set of data obtained in this study in different cell types and in clonal cell populations suggests that a complexity of events is involved in the formation and maintenance of abnormal sequence patterns, which correspond to the same genomic position of cancer rearrangements (Durkin et al., 2008). To the best of our knowledge, this study reports the first direct observation of recurrent instability at *FHIT* in normal human cells. Remarkably, the same sequence abnormalities would remain undetected or not interpreted through genome-wide analyses, because of their low frequency and heterogeneity. Therefore, molecular combing is confirmed as a valuable tool integrating high-resolution single-locus sequence analysis with a quantitative approach.

FRA3B is the most active fragile site of the human genome, and this could have improved the chance to observe rare events of spontaneous instability which are otherwise neglected. On the other hand, extremely rare events may have great impact when involving critical gene functions, and direct findings are now provided for the impact of somatic mosaicism in cancer etiology (Jacobs et al., 2012; Laurie et al., 2012). In the light of the potential relevance of fragile sites for human disease, the present results deserve great attention.

ACKNOWLEDGMENTS

We are grateful to F. Pacchierotti (ENEA, CR Casaccia, Italy) and to A. Vezzi (Department of Biology, University of Padova) for their precious advice in the course of the study.

References

Becker NA, Thorland EC, Denison SR, Phillips LA, Smith DI. 2002. Evidence that instability within the FRA3B region extends four megabases. Oncogene 21:8713–8722.

Bermejo R, Lai MS, Foiani M. 2012. Preventing replication stress to maintain genome stability: Resolving conflicts between replication and transcription. Mol Cell 45:710–718.

Bignell GR, Greenman CD, Davies H, Butle AP, Edkins S, Andrews JM, Buck G, Chen L, Beare D, Latimer C, Widaa S, Hinton J, Fahey C, Fu B, Swamy S, Dalgliesh GL, The BN, Deloukas P, Yang F,.Campbell PJ, Futreal PA, Stratton MR. 2010. Signatures of mutation and selection in the cancer genome. Nature 463:893–898.

Branzei D, Foiani M. 2010. Maintaining genome stability at the replication fork. Nat Rev Mol Cell Biol 11:208–219.

Caporossi D, Vernole P, Nicoletti B, Tedeschi B. 1995. Characteristic chromosomal fragility of human embryonic cells exposed in vitro to aphidicolin. Hum Genet 96:269–274.

Debatisse M, Le Tallec B, Letessier A, Dutrillaux B, Brison O. 2012. Common fragile sites: Mechanisms of instability revisited. Trends Genet 28:22–32.

Druck T, Hadaczek P, Fu TB, Ohta M, Siprashvili Z, Baffa R, Negrini M, Kastury K, Veronese ML, Rosen D, Rothstein J, McCue P, Cotticelli MG, Inoue H, Croce CM, Huebner K. 1997. Structure and expression of the human FHIT gene in normal and tumor cells. Cancer Res 57:504–512.

Durkin SG, Glover TW. 2007. Chromosome fragile sites. Annu Rev Genet 41:169–192.

Durkin SG, Ragland RL, Arlt MF, Mulle JG, Warren ST Glover TW. 2008. Replication stress induces tumor-like microdeletions in FHIT/FRA3B. Proc Natl Acad Sci USA 105:246–251.

Gayther SA, Barski P, Batley SJ, Li L, de Foy KAF, Cohen SN, Ponder BAJ, Caldas C. 1997. Aberrant splicing of the TSG101 and FHIT genes occurs frequently in multiple malignancies and in normal tissues and mimics alterations previously described in tumours. Oncogene 15:2119–2126.

Hastings PJ, Ira G, Lupski JR. 2009. A microhomology-mediated break-induced replication model for the origin of human copy number variation. PLoS Genet 5:e1000327.

Helmrich A, Ballarino M, Tora L. 2011. Collisions between replication and transcription complexes cause common fragile site instability at the longest human genes. Mol Cell 44:966–977.

Jacobs KB, Yeager M, Zhou W, Wacholder S, Wang Z, Rodriguez-Santiago B, Hutchinson A, Deng X, Liu C, Horner MJ, Cullen M, Epstein CG, Burdett L, Dean MC, Chatterjee N, Sampson J, Chung CC, Kovaks J, Gapstur SM, Stevens VL, Teras LT, Gaudet MM, Albanes D, Weinstein SJ, Virtamo J, Taylor PR, Freedman ND, Abnet CC, Goldstein AM, Hu N, Yu K, Yuan JM, Liao L, Ding T, Qiao YL, Gao YT, Koh WP, Xiang YB, Tang ZZ, Fan JH, Aldrich MC, Amos C, Blot WJ, Bock CH, Gillanders EM, Harris CC, Haiman CA, Henderson BE, Kolonel LN, Le Marchand L, McNeill LH, Rybicki BA, Schwartz AG, Signorello LB, Spitz MR, Wiencke JK, Wrensch M, Wu X, Zanetti KA, Ziegler RG, Figueroa JD, Garcia-Closas M, Malats N, Marenne G, Prokunina-Olsson L, Baris D, Schwenn M, Johnson A, Landi MT, Goldin L, Consonni D, Bertazzi PA, Rotunno M, Rajaraman P, Andersson U, Beane Freeman LE, Berg CD, Buring JE, Butler MA, Carreon T, Feychting M, Ahlbom A, Gaziano JM, Giles GG, Hallmans G, Hankinson SE, Hartge P, Henriksson R, Inskip PD, Johansen C, Landgren A, McKean-Cowdin R, Michaud DS, Melin BS, Peters U, Ruder AM, Sesso HD, Severi G, Shu XO, Visvanathan K, White E, Wolk A, Zeleniuch-Jacquotte A, Zheng W, Silverman DT, Kogevinas M, Gonzalez JR, Villa O, Li D, Duell EJ, Risch HA, Olson SH, Kooperberg C, Wolpin BM, Jiao L, Hassan M, Wheeler W, Arslan AA, Bueno-de-Mesquita HB, Fuchs CS, Gallinger S, Gross MD, Holly EA, Klein AP, LaCroix A, Mandelson MT, Petersen G, Boutron-Ruault MC, Bracci PM, Canzian F, Chang K, Cotterchio M, Giovannucci EL, Goggins M, Hoffman Bolton JA, Jenab M, Khaw KT, Krogh V, Kurtz RC, McWilliams RR, Mendelsohn JB, Rabe KG, Riboli E, Tjønneland A, Tobias GS, Trichopoulos D, Elena JW, Yu H, Amundadottir L, Stolzenberg-Solomon RZ, Kraft P, Schumacher F, Stram D, Savage SA, Mirabello L, Andrulis IL, Wunder JS, Patiño García A, Sierrasesúmaga L, Barkauskas DA, Gorlick RG, Purdue M, Chow WH, Moore LE, Schwartz KL, Davis FG, Hsing AW, Berndt SI, Black A, Wentzensen N, Brinton LA, Lissowska J, Peplonska B, McGlynn KA, Cook MB, Graubard BI, Kratz CP, Greene MH, Erickson RL, Hunter DJ, Thomas G, Hoover RN, Real FX, Fraumeni JF Jr, Caporaso NE, Tucker M, Rothman N, Pérez-Jurado LA, Chanock SJ. 2012. Detectable clonal mosaicism and its relationship to aging and cancer. Nature Genet 44:651–658.

Lai LA, Kostadinov R, Barrett MT, Peiffer DA, Pokholok D, Odze R, Sanchez CA, Maley CC, Reid BJ, Gunderson KL, Rabinovitch PS. 2010. Deletion at fragile sites is a common and early event in Barrett's esophagus. Mol Cancer Res 8:1084–1094.

Lambert S, Carr AM. 2013. Impediments to replication fork movement: stabilisation, reactivation and genome instability. Chromosoma 122:33–45.

Laurie CC, Laurie CA, Rice K, Doheny KF, Zelnick LR, McHugh CP, Ling H, Hetrick KN, Pugh EW, Amos C, Wei Q, Wang LE, Lee JE, Barnes KC, Hansel NN, Mathias R, Daley D, Beaty TH, Scott AF, Ruczinski I, Scharpf RB, Bierut LJ, Hartz SM, Landi MT, Freedman ND, Goldin LR, Ginsburg D, Li J, Desch KC, Strom SS, Blot WJ, Signorello LB, Ingles SA, Chanock SJ, Berndt SI, Le Marchand L, Henderson BE, Monroe KR, Heit JA, de Andrade M, Armasu SM, Regnier C, Lowe WL, Hayes MG, Marazita ML, Feingold E, Murray JC, Melbye M, Feenstra B, Kang JH, Wiggs JL, Jarvik GP, McDavid AN, Seshan VE, Mirel DB, Crenshaw A, Sharopova N, Wise A, Shen J, Crosslin DR, Levine DM, Zheng X, Udren JI, Bennett S, Nelson SC, Gogarten SM, Conomos MP, Heagerty P, Manolio T, Pasquale LR, Haiman CA, Caporaso N, Weir BS. 2012. Detectable clonal mosaicism from birth to old age and its relationship to cancer. Nature Genet 44:642–650.

Le Beau MM, Rassool FV, Neilly ME, Espinosa R3rd, Glover TW, Smith DI, McKeithan TW. 1998. Replication of a common fragile site, FRA3B, occurs late in S phase and is delayed further upon induction: Implications for the mechanism of fragile site induction. Hum Mol Genet 7:755–761.

Letessier A, Millot GA, Koundrioukoff S, Lachages AM, Vogt N, Hansen RS, Malfoy B, Brison O, Debatisse M. 2011. Cell-type-specific replication initiation programs set fragility of the FRA3B fragile site. Nature 470:120–123.

Matthews CP, Shera K, Kiviat N, McDougall JK. 2001. Expression of truncated FHIT transcripts in cervical cancers and in normal human cells. Oncogene 20:4665–4675.

Michalet X, Ekong R, Fougerousse F, Rousseaux S, Schurra C, Hornigold N, van Slegtenhorst M, Wolfe J, Povey S, Beckmann JS, Bensimon A. 1997. Dynamic molecular combing: Stretching the whole human genome for high-resolution studies. Science 277:1518–1523.

Murano I, Juwano A, Kajii T. 1989. Fibroblast-specific common fragile sites induced by aphidicolin. Hum Genet 8:45–48.

Ohta M, Inoue H, Cotticelli MG, Kastury K, Baffa R, Palazzo J, Siprashvili Z, Mori M, McCue P, Druck T, Croce CM, Huebner K. 1996. The FHIT gene, spanning the chromosome 3p14.2 fragile site and renal carcinoma-associated t(3;8) breakpoint, is abnormal in digestive tract cancers. Cell 84: 587–597.

Okumura H, Ishii H, Pichiorri F, Croce CM, Mori M, Huebner K. 2009. Fragile gene product, Fhit, in oxidative and replicative stress responses. Cancer Sci 100:1145–1150.

Palakodeti A, Lucas I, Jiang Y, Young DJ, Fernald AA, Karrison T, Le Beau MM. 2010. Impaired replication dynamics at the FRA3B common fragile site. Hum Mol Genet 19:99–110.

Palumbo E, Matricardi L, Tosoni E, Bensimon A, Russo A. 2010. Replication dynamics at common fragile site FRA6E. Chromosoma 119:575–587.

Panagopoulos I, Thelin S, Mertens F, Mitelman F, Aman P. 1997. Variable FHIT transcripts in non-neoplastic tissues. Genes Chrom. Cancer 19:215–219.

Pichiorri F, Ishii H, Okumura H, Trapasso F, Wang Y, Huebner K. 2008. Molecular parameters of genome instability: roles of fragile genes at common fragile sites. J Cell Biochem 104:1525–1533.

Rassool FV, Le Beau MM, Shen ML, Neilly ME, Espinosa R3rd, Ong ST, Boldog F, Drabkin H, McCarroll R, McKeithan TW. 1996. Direct cloning of DNA sequences from the common fragile site region at chromosome band 3p14.2. Genomics 35:109–117.

Saldivar JC, Shibata H, Huebner K. 2010. Pathology and biology associated with the fragile FHIT gene and gene product. J Cell Biochem 109:858–865.

Saldivar JC, Miuma S, Bene L, Hosseini SA, Shibata H, Sun J, Wheeler LJ, Mathews CK, Huebner K. 2012. Initiation of genome instability and preneoplastic processes through loss of Fhit expression. PLoS Genet. 8:e1003077.

Smith DI, Zhu Y, McAvoy S, Kuhn R. 2006. Common fragile sites, extremely large genes, neural development and cancer. Cancer Lett 232:48–57.

Smith CE, Llorente B, Symington LS. 2007. Template switching during break-induced replication. Nature 447:102–105.

Stein CK, Glover TW, Palmer JL, Glisson BS. 2002. Direct Correlation Between *FRA3B* expression and Cigarette Smoking. Genes Chrom Cancer 34:333–340.

Wang L, Darling J, Zhang JS, Huang H, Liu W, Smith DI. 1999. Allele-specific late replication and fragility of the most active common fragile site, FRA3B. Hum Mol Genet 8:431–437.

Yunis JJ and Soreng AL. 1984. Constitutive fragile sites and cancer. Science 226:1199–1204.

Zimonjic DB, Druck T, Ohta M, Kastury K, Croce CM, Popescu NC, Huebner K. 1997. Positions of chromosome 3p14.2 fragile sites (FRA3B) within the FHIT gene. Cancer Res 57:1166–1170.